# Dynamics of quantum coherence and quantum Fisher information after a sudden quench

R. Jafari [1,2,3,*] and Alireza Akbari [4,5,1,†]

[1]*Department of Physics, Institute for Advanced Studies in Basic Sciences (IASBS), Zanjan 45137-66731, Iran*

[2]*Department of Physics, University of Gothenburg, SE 412 96 Gothenburg, Sweden*

[3]*Beijing Computational Science Research Center, Beijing 100094, China*

[4]*Max Planck Institute for the Chemical Physics of Solids, D-01187 Dresden, Germany*

[5]*Max Planck POSTECH Center for Complex Phase Materials, and Department of Physics, POSTECH, Pohang, Gyeongbuk 790-784, Korea*

(Received 12 February 2020; accepted 13 May 2020; published 8 June 2020)

The dynamics of relative entropy and $l_1$ norm of coherence, as well as, the Wigner-Yanase skew and quantum Fisher information are studied in the one-dimensional $XY$ spin chain in the presence of a time-dependent transverse magnetic field. We show that, independent of the initial state of the system and while the relative entropy of coherence, the $l_1$ norm of coherence, and quantum Fisher information are incapable, surprisingly, the Wigner-Yanase skew information dynamic can truly spotlight the equilibrium critical point. We also observe that, when the system is quenched to the critical point, these quantities show suppressions and revivals. Moreover, the first suppression (revival) time scales linearly with the system size and its scaling ratio is unique for all quenches independent of the initial phase of the system. This is the promised universality of the first suppression (revival) time.

DOI: 10.1103/PhysRevA.101.062105

## I. INTRODUCTION

Evaluating quantum coherence (QC) is highly substantial for both quantum foundations and quantum technologies [1,2]. Quantum coherence itself represents an essential feature of quantum states and supports all forms of quantum correlations [3]; however, the inevitable interaction of the system with the environment mostly brings incoherency to the input states and evolves a coherence loss [4]. Recently, several precise measures have been introduced to quantify the quantum coherence [5–8], including the $l_1$ norm quantum coherence ($Cl_1$) [5,9], the relative entropy of coherence (REC) [5], the trace norm quantum coherence (TQC) [5,10] and the Wigner-Yanase skew information (WYSI) [11]. Among these quantum resource measures, TQC and $Cl_1$ are defined through a well trace norm, where a closed analytical formula for calculating $X$ states has been derived invariant under unitary transformations [10,12–15]. Skew information was first introduced by Wigner and Yanase in 1963 [16] and was originally used to represent the information content of mixed states. In the theory of statistical estimation, the statistical idea that governs skew information is Fisher information [17], which is not only a key notion of statistical inference [18] but also plays an important role in informational treatments of physics [19–21].

Nowadays, quantum Fisher information (QFI), as a witness of multipartite entanglement, displays much richer aspects of complex structures of topological states [22]. It has been extensively explored in many different fields such as the calculation of quantum speedup limit time [23], the study of uncertainty relations [24,25], and the properties of quantum phase transition [26,27]. In particular, quantum Fisher information prepares a bound to characterize the members of a family of probability distributions. Moreover, when quantum systems are involved, an excellent measurement may be found by using tools from quantum estimation theory. This is especially true for a kind of problems for which the quantity of interest is not directly available.

Quantum Fisher information has introduced the quantum version of the Cramér-Rao inequality [19,28–30] and has imposed the lower bound [29]. Moreover, different features of quantum coherence have been studied, including quantification, dynamic evolution, and operational explanation of quantum coherence [7,31–34]. Some recent works have also examined the relationship between quantum coherence and quantum phase transition [25–27], as well as the performance of the quantum walk version of the Deutsch-Jozsa algorithm and the deterministic quantum computation with one quantum bit (DQC1) algorithm [35–37]. Additionally, it has been shown that multipartite entanglement which witnessed by QFI can capture a quantum phase-transition point [29,38]. However, despite several works on quantum coherence and QFI, the dynamics of quantum coherence and QFI have not yet been studied sufficiently. Therefore, understanding dynamical behavior of quantum coherence and QFI would be very useful for the description of the nonequilibrium dynamics and universal behavior of quantum many-body systems [39–49].

In this paper, by considering a one-dimensional $XY$ model with time-dependent (step function) couplings in an external time-dependent (step function) transverse magnetic field, we study the dynamical behavior of the relative entropy of coherence, $l_1$ norm of coherence, and also as measures of quantum coherence, the Wigner-Yanase skew and quantum Fisher information. We find that all of these quantities show

*rohollah.jafari@gmail.com

†akbari@postech.ac.kr

 

suppressions and revivals when the system is quenched to the critical point. We also show that the first suppression (revival) time scales linearly with the system size. This scaling ratio is independent of the size of the quench and the initial preparation phase of the system.

## II. TIME-DEPENDENT *XY* MODEL

The Hamiltonian of the time-dependent $XY$ model in a one-dimensional lattice is given by [50–53]

$$\mathcal{H} = -\sum_{i=1}^{N}\left[J(t)\left[(1+\gamma)S_i^x S_{i+1}^x + (1-\gamma)S_i^y S_{i+1}^y\right] + h(t)S_i^z\right], \tag{1}$$

where $N$ shows the site's number, and $\gamma$ is the anisotropy parameter. We consider the periodic boundary condition and $S_i^\alpha$ are the spin-half operators at the $i$th site, which are defined by half of the Pauli matrices as follows

$$S_i^\alpha = \tfrac{1}{2}\sigma_i^\alpha, \quad \alpha = \{x, y, z\}.$$

To study the effect of a time-varying coupling parameter $J(t)$ and magnetic field $h(t)$, we assume the following expressions:

$$\begin{aligned} J(t) &= J_0 + (J_1 - J_0)\Theta(t), \\ h(t) &= h_0 + (h_1 - h_0)\Theta(t), \end{aligned} \tag{2}$$

with the Heaviside step function defined by

$$\Theta(t) = \begin{cases} 0 & t \leqslant 0 \\ 1 & t > 0. \end{cases} \tag{3}$$

The considered model (1) can be exactly diagonalized by standard Jordan-Wigner transformation [50–54]. Then the Liouville equation of the Fourier-transformed Hamiltonian can be solved exactly and the magnetization and two-point correlation functions can be calculated analytically [50–54].

In the subsequent calculations, we assume that the system is initially at thermal equilibrium. In this respect, the reduced two-spin density matrix $\varrho_{l,m}(t)$ is achieved by

$$\varrho_{l,m}(t) = \begin{pmatrix} \rho_{11} & 0 & 0 & \rho_{14} \\ 0 & \rho_{22} & \rho_{23} & 0 \\ 0 & \rho_{23}^* & \rho_{33} & 0 \\ \rho_{14}^* & 0 & 0 & \rho_{44} \end{pmatrix}, \tag{4}$$

where its matrix elements can be written in terms of one- and two-point correlation functions, which are given by

$$\begin{aligned} \rho_{11} &= \langle M_l^z\rangle + \langle S_l^z S_m^z\rangle + \tfrac{1}{4}, \quad \rho_{22} = \rho_{33} = -\langle S_l^z S_m^z\rangle + \tfrac{1}{4}, \\ \rho_{23} &= \langle S_l^x S_m^x\rangle + \langle S_l^y S_m^y\rangle, \quad \rho_{14} = \langle S_l^x S_m^x\rangle - \langle S_l^y S_m^y\rangle, \\ \rho_{44} &= -\langle M_l^z\rangle + \langle S_l^z S_m^z\rangle + \tfrac{1}{4}, \end{aligned} \tag{5}$$

with the magnetization in the $z$ direction characterized as follows:

$$M^z = \frac{1}{N}\sum_{j=1}^{N} M_j^z = \frac{1}{N}\sum_{j=1}^{N} S_j^z. \tag{6}$$

Here, the expectation for the average value is defined by

$$\langle\cdots\rangle = \frac{\mathrm{Tr}[(\cdots)\rho(t)]}{\mathrm{Tr}[\rho(t)]}, \tag{7}$$

where the exact analytical form of the magnetization, and two-point spin-spin correlation functions are precisely presented in Refs. [50–54] (see also Appendix A).

## III. QUANTUM COHERENCE AND QUANTUM FISHER INFORMATION

As mentioned, quantum coherence is a fundamental physical resource in quantum information tasks [55], and revealing quantum coherence is imperative to accomplish the realization of the quantum correlations. It is understood as a key root for physical resources in quantum computation and quantum information processing, and a rigorous theory has been proposed to define an excellent notion for measuring it [5]. In this section we briefly quantify and review the relative entropy of coherence, $l_1$ norm of coherence, Wigner-Yanase skew information, and quantum Fisher information.

### A. The relative entropy and $l_1$ norm of coherence

The $l_1$ norm of coherence is defined as a sum of the absolute values of all off-diagonal elements in the density matrix $\varrho_{l,m}$ using following expression [5]:

$$\mathrm{C}l_1(\varrho) = \sum_{l\neq m} |\varrho_{l,m}|. \tag{8}$$

Moreover, the relative entropy of coherence is defined as

$$\mathrm{C}_{\mathrm{REC}}(\varrho) = S(\varrho_{\mathrm{diag}}) - S(\varrho), \tag{9}$$

where $\varrho_{\mathrm{diag}}$ is the diagonal part of $\varrho_{l,m}$, and the function

$$S(\varrho_{l,m}) = -\mathrm{Tr}[\varrho_{\mathrm{l,m}}\log_2\varrho_{\mathrm{l,m}}] \tag{10}$$

is the von Neumann entropy of the density matrix $\varrho_{l,m}$. Calculating the $l_1$ norm for a transverse field $XY$ model is straightforward and results in

$$\mathrm{C}l_1 = 4\left|\langle S_l^x S_m^x\rangle\right|. \tag{11}$$

Furthermore, using the relative entropy formula (9), we have

$$\mathrm{C}_{\mathrm{REC}} = \sum_{q=0}^{1}(\xi_q\log_2\xi_q + \eta_q\log_2\eta_q - \zeta_q\log_2\zeta_q) - 2\varepsilon\log_2\varepsilon, \tag{12}$$

with

$$\begin{aligned} \xi_q &= \tfrac{1}{4} - \langle S_l^z S_m^z\rangle + (-1)^q\left(\langle S_l^x S_m^x\rangle + \langle S_l^y S_m^y\rangle\right), \\ \eta_q &= \tfrac{1}{4} + \langle S_l^z S_m^z\rangle + (-1)^q\sqrt{\langle S_l^z\rangle^2 + \left(\langle S_l^x S_m^x\rangle - \langle S_l^y S_m^y\rangle\right)^2}, \\ \varepsilon &= \tfrac{1}{4} - \langle S_l^z S_m^z\rangle. \end{aligned} \tag{13}$$

### B. The Wigner-Yanase skew information

The definition of the Wigner-Yanase skew information which is used as a measure of quantum coherence is given by [11,16,25,56]

$$I(\varrho, V) = -\tfrac{1}{2}\mathrm{Tr}[\sqrt{\varrho}, V]^2, \tag{14}$$

where the density matrix $\varrho$ depicts a mixed quantum state, $V$ is an observable, and $[\cdots,\cdots]$ represents the commutator. The quantity $I(\varrho, V)$ can also be interpreted as a measure of the quantum uncertainty of $V$ in the state $\varrho$ instead of

the conventional variance. A set of the local spin's elements ($S^\alpha$) is an arbitrary and natural choice of observable which constitutes a local orthonormal basis, as

$$\mathrm{LQC}_\alpha = I\big(\varrho_{l,m}, S_l^\alpha \otimes \mathbb{1}_m\big). \tag{15}$$

The reduced two-spin density matrix (4) facilitates the analytical evaluation of the Wigner-Yanase skew information of the two-spin density matrix. Thus, one can obtain the eigenvalues and their corresponding normalized eigenvectors of the density matrix as

$$\begin{aligned}
p_1 &= \tfrac{1}{2}(\rho_{11}+\rho_{44}+\sqrt{(\rho_{11}-\rho_{44})^2+4|\rho_{14}|^2}),\\
p_2 &= \tfrac{1}{2}(\rho_{11}+\rho_{44}-\sqrt{(\rho_{11}-\rho_{44})^2+4|\rho_{14}|^2}),\\
p_3 &= \tfrac{1}{2}(\rho_{22}+\rho_{33}+\sqrt{(\rho_{22}-\rho_{33})^2+4|\rho_{23}|^2}),\\
p_4 &= \tfrac{1}{2}(\rho_{22}+\rho_{33}-\sqrt{(\rho_{22}-\rho_{33})^2+4|\rho_{23}|^2}),
\end{aligned} \tag{16}$$

and

$$\begin{aligned}
|\phi_1\rangle &= \frac{1}{N_1}\begin{pmatrix}\rho_{14}\\0\\0\\p_1-\rho_{11}\end{pmatrix}, \quad |\phi_2\rangle = \frac{1}{N_2}\begin{pmatrix}\rho_{14}\\0\\0\\p_2-\rho_{11}\end{pmatrix},\\
|\phi_3\rangle &= \frac{1}{N_3}\begin{pmatrix}0\\\rho_{23}\\p_3-\rho_{22}\\0\end{pmatrix}, \quad |\phi_4\rangle = \frac{1}{N_4}\begin{pmatrix}0\\\rho_{23}\\p_4-\rho_{22}\\0\end{pmatrix},
\end{aligned} \tag{17}$$

respectively. Here $N_i$ $(i=1,2,3,4)$ are the normalization factors and are defined by

$$\begin{aligned}
N_1 &= \sqrt{|\rho_{14}|^2+(p_1-\rho_{11})^2}, \quad N_2 = \sqrt{|\rho_{14}|^2+(p_2-\rho_{11})^2},\\
N_3 &= \sqrt{|\rho_{23}|^2+(p_3-\rho_{22})^2}, \quad N_4 = \sqrt{|\rho_{23}|^2+(p_4-\rho_{22})^2}.
\end{aligned} \tag{18}$$

By straightforward calculations, the root of the two-qubit reduced state, $\sqrt{\varrho_{l,m}}$, can be obtained as

$$\sqrt{\varrho_{l,m}} = \begin{pmatrix}\alpha_\varrho & 0 & 0 & \lambda_\varrho\\ 0 & \beta_\varrho & \nu_\varrho & 0\\ 0 & \nu_\varrho^* & \gamma_\varrho & 0\\ \lambda_\varrho^* & 0 & 0 & \delta_\varrho\end{pmatrix}, \tag{19}$$

with the following elements:

$$\begin{aligned}
\alpha_\varrho &= |\rho_{14}|^2\left(\frac{\sqrt{p_1}}{N_1^2}+\frac{\sqrt{p_2}}{N_2^2}\right),\\
\beta_\varrho &= |\rho_{23}|^2\left(\frac{\sqrt{p_3}}{N_3^2}+\frac{\sqrt{p_4}}{N_4^2}\right),\\
\gamma_\varrho &= \frac{\sqrt{p_3}(p_3-\rho_{22})^2}{N_3^2}+\frac{\sqrt{p_4}(p_4-\rho_{22})^2}{N_4^2},\\
\delta_\varrho &= \frac{\sqrt{p_1}(p_1-\rho_{11})^2}{N_1^2}+\frac{\sqrt{p_2}(p_2-\rho_{11})^2}{N_2^2},\\
\lambda_\varrho &= \rho_{14}\left(\frac{\sqrt{p_1}(p_1-\rho_{11})}{N_1^2}+\frac{\sqrt{p_2}(p_2-\rho_{11})}{N_2^2}\right),\\
\nu_\varrho &= \rho_{23}\left(\frac{\sqrt{p_3}(p_3-\rho_{11})}{N_3^2}+\frac{\sqrt{p_4}(p_4-\rho_{11})}{N_4^2}\right).
\end{aligned} \tag{20}$$

In addition, for the bipartite system in Eq. (4), the two-spin local quantum coherence (LQC) components can be written as [57]

$$\begin{aligned}
\mathrm{LQC}_x &= 1-2(\alpha_\varrho\beta_\varrho+\gamma_\varrho\delta_\varrho)-4\mathrm{Re}[\lambda_\varrho\nu_\varrho],\\
\mathrm{LQC}_y &= 1-2(\alpha_\varrho\beta_\varrho+\gamma_\varrho\delta_\varrho)+4\mathrm{Re}[\lambda_\varrho\nu_\varrho],\\
\mathrm{LQC}_z &= 1-\big[\alpha_\varrho^2+\beta_\varrho^2+\gamma_\varrho^2+\delta_\varrho^2-2(|\lambda_\varrho|^2+|\nu_\varrho|^2)\big],
\end{aligned} \tag{21}$$

which quantify the coherence with respect to the first subsystem locally.

### C. The Quantum Fisher information

Estimation theory is an important topic in different areas of physics [19,28,38,58–60]. In the general phase-estimation perspective, the evolution of a mixed quantum state, given by the density matrix $\varrho$, under a unitary transformation, can be described as

$$\varrho_\theta = e^{-iA\theta}\varrho e^{iA\theta}, \tag{22}$$

where $\theta$ is the phase shift and $A$ is an operator. The estimation accuracy for $\theta$ is bounded by the quantum Cramér-Rao inequality [19,28]:

$$\Delta\hat{\theta} \geqslant \frac{1}{\sqrt{\nu\mathcal{F}(\varrho_\theta)}}, \tag{23}$$

where $\hat{\theta}$ expresses the unbiased estimator for $\theta$, and $\nu$ is the number of times the measurement is repeated. Correspondingly, $\mathcal{F}(\varrho_\theta)$ is the so-called quantum Fisher information, which is defined as [19,28,59,60]

$$\mathcal{F}(\varrho,A) = 2\sum_{m,n}\frac{(p_m-p_n)^2}{(p_m+p_n)}|\langle m|A|n\rangle|^2, \tag{24}$$

where $p_m$ and $|\phi_m\rangle$ represent the eigenvalues and eigenvectors of the density matrix $\varrho$, respectively. Now, following the route provided in Ref. [57], the quantum Fisher information can be written as

$$\mathcal{F}_Q = \sum_\mu \mathcal{F}(\varrho, A_\mu\otimes I + I\otimes B_\mu), \tag{25}$$

where $\{A_\mu\}$ and $\{B_\mu\}$ are arbitrary and natural complete sets of local orthonormal observables of the two subsystems with

respect to $\varrho$. The value of $\mathcal{F}_Q$ given by Eq. (25) is independent of the choice of local orthonormal bases [57], meaning that it is an inherent quantity of the composite system. For a general two-spin system, the local orthonormal observables $\{A_\mu\}$ and $\{B_\mu\}$ can be defined as

$$\{A_\mu\} = \{B_\mu\} = \sqrt{2}\{I, S^x, S^y, S^z\}, \tag{26}$$

and finally, for the reduced two-spin density matrix in Eq. (4) the analytical evaluation of the QFI can be evaluated as

$$\begin{aligned}\mathcal{F}_Q = {} & \frac{16\left(\langle S_i^x S_{i+r}^x\rangle - \langle S_i^y S_{i+r}^y\rangle\right)^2}{1+4\langle S_i^z S_{i+r}^z\rangle} \\ & + \left[\frac{16}{\left(1+4\langle S_i^x S_{i+r}^x\rangle\right)\left(1+4\langle S_i^y S_{i+r}^y\rangle\right)-4\langle S_i^z\rangle^2}\right] \\ & \times \Big[\left(3\langle S_i^z\rangle^2+4\langle S_i^z S_{i+r}^z\rangle^2-2\langle S_i^z S_{i+r}^z\rangle\right)\left(\langle S_i^x S_{i+r}^x\rangle\right. \\ & \left.+\langle S_i^y S_{i+r}^y\rangle\right)+\frac{1}{2}\left(\langle S_i^z\rangle^2+4\langle S_i^z S_{i+r}^z\rangle^2-8\langle S_i^z\rangle^2\langle S_i^z S_{i+r}^z\rangle\right) \\ & +\left(1-8\langle S_i^z S_{i+r}^z\rangle\right)\left(\langle S_i^x S_{i+r}^x\rangle^2+\langle S_i^y S_{i+r}^y\rangle^2\right) \\ & +4\langle S_i^x S_{i+r}^x\rangle^3+4\langle S_i^y S_{i+r}^y\rangle^3\Big].\end{aligned} \tag{27}$$

## IV. NUMERICAL RESULTS AND DISCUSSIONS

We now come to present our numerical results. Although our formalism was for a general case, for simplicity we restrict our discussion to the time-dependent transverse magnetic field, i.e., $J_1 = J_0 = 1$. Furthermore, in the main text we only consider a time-dependent transverse field Ising model (TFIM) by setting $\gamma = 1$, and for more general cases, $\gamma \neq 1$, one can look at Appendix B. It is well known that the ground state of the TFIM is characterized by a quantum phase transition that takes place at the critical point $h_c = J_0$ [61,62]. This phase transition is a result of the quantum fluctuations at zero temperature, which destroy the quantum correlations in the ground state. It is determined via the order parameter $\langle M^x\rangle$, which differs from a finite value for $h < h_c$ to zero for $h \geqslant h_c$.

Moreover, the ground state is ferromagnetic aligned in the $x$ direction for zero magnetic field and it has a paramagnetic alignment along the field for the limit of large magnetic field. Both cases are minimally entangled since the ground state is a product of individual spin states pointing in the $z$ ($x$) direction as $h \to \infty$ ($h \to 0$) [61,62]. Furthermore, by raising the temperature, the entanglement shows a sudden decay near the critical point, although it remains constant at zero temperature and in the vicinity of the critical point [63].

### A. Quench away from the critical point

In Fig. 1(a), we plot the intensity of the relative entropy of coherence, the $l_1$ norm of coherence [Fig. 1(b)], the quantum Fisher information [Fig. 1(c)], and local quantum coherence components [Figs. 1(d)–1(f)], versus $t$ and $h_1$. The plots are for $h_0 = 0.7$, and at zero temperature. As one can see, for zero $h_1$, where the spins are completely aligned in the $x$ direction, all quantities (expect $\mathrm{Cl}_1$) show an oscillatory behavior in time. By introducing an external magnetic field $h_1$, the

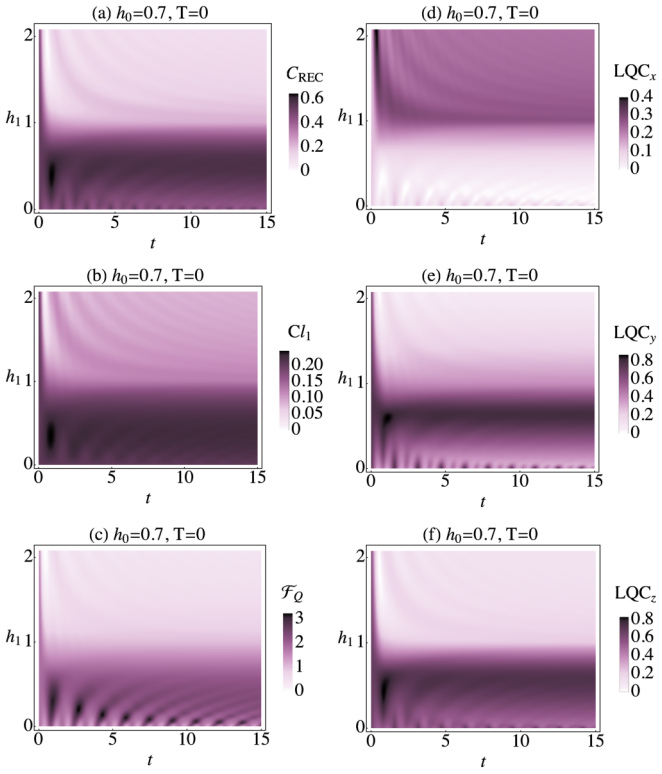


FIG. 1. Density plots of (a) the relative entropy of quantum coherence ($\mathrm{C_{REC}}$), (b) the $l_1$ norm of quantum coherence ($\mathrm{Cl}_1$), (c) the quantum Fisher information (QFI), and (d)–(f) the local quantum coherence ($\mathrm{LQC}_\alpha$) with $\alpha = x, y, z$, versus $t$ and $h_1$, at zero temperature and for $h_0 = 0.7$ ($h_0 < h_c$).

magnitude of quantities increases as the field increases until they reach their maximum value close to $h_1^M = h_1 \approx 0.5$. In different circumstances, the maximum values of $\mathrm{LQC}_x$ occur at the equilibrium critical point $h_1^M = h_1 = h_c$. As $h_1$ exceeds $h_1^M$, the magnitude of all quantities decreases gradually by magnetic field. Thus, when the system initially is prepared in the ferromagnetic phase, $M^x(t, T = 0) \neq 0$, the maximum of two-spin $S^x$ local coherence occurs at the equilibrium critical point and $\mathrm{LQC}_x$ is the only quantity that can capture truly the critical point. It should be mentioned that, when the system is prepared in its critical point, $h_0 = h_c$, the maximum value that quantities can reach is much greater than in the previous case and appears at $h_1^M = h_1 = h_c$.

To further elaborate on the behavior of the zero-temperature dynamics above the transition field, $h_0 > h_c$, Fig. 2(a) presents the intensity of the relative entropy of coherence, the $l_1$ norm of coherence [Fig. 2(b)], the quantum Fisher information [Fig. 2(c)], and local quantum coherence components [Figs. 2(d)–2(f)], versus $t$ and $h_1$. We assume $h_0 = 1.5$, where the system is initially prepared in the paramagnetic phase, $M^z(t, T = 0) \neq 0$. As seen, for $h_1 = 0$, all quantities show an oscillatory behavior in time. Besides, when the external magnetic field is turned on ($h_1 > 0$), the magnitude of all quantities except $\mathrm{LQC}_x$ and $\mathrm{LQC}_y$ enhances until reaching a maximum value at the equilibrium critical point $h_1^M = h_1 = h_c$, then reduces upon increasing the magnetic field. From these findings one can conclude that dynamical two-spin local $S^z$, quantum coherence (WYSI), can positively

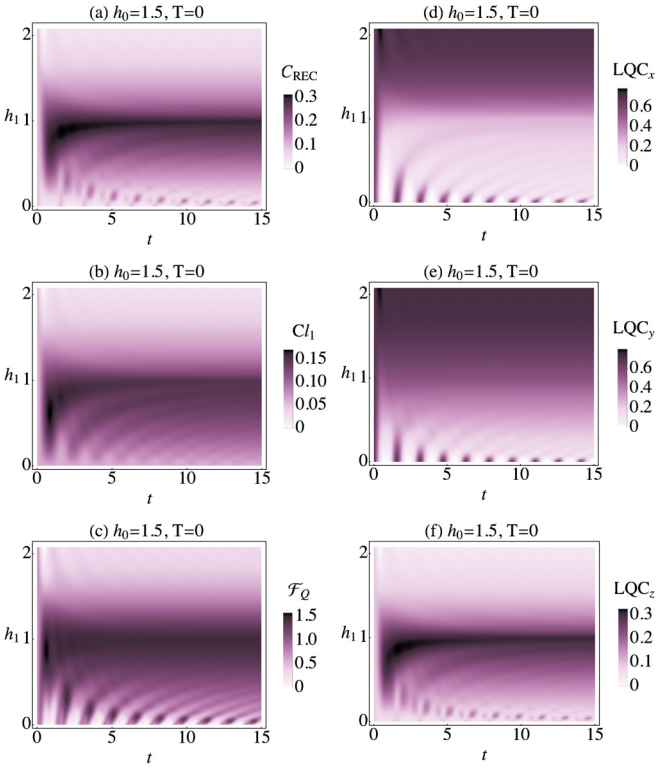


FIG. 2. Same density plots as in Fig. 1 but for the case of $h_0 = 1.5$ ($h_0 > h_c$).

pick out the critical point while the REC, QFI, and $Cl_1$ fail in this task. To summarize, it depends on the initial state which the system is prepared, dynamics of the proper component of local quantum coherence can capture the critical point of the system. In other words, when the system is prepared in the initial state with $M^\alpha \neq 0$, the dynamics of $LQC_\alpha$ reaches its maximum value at the critical point.

On top of that, there would be a great interest to study the effect of temperature on the critical behavior of many-body systems such as the spin systems [63–66]. To show whether the WYSI is able to pinpoint the critical point at finite temperature, we plot the $LQC_x$ and $LQC_z$ in Fig. 3 for different temperatures; namely, $T = 1$ and $T = 5$. Although the maximum value of LQC decreases as the temperature increases, the equilibrium phase transition point can still be signalled by the maximum of $LQC_x$ and $LQC_z$ at low temperature. This significant property can be easily applied to determine quantum critical points of the systems which today's technology makes it virtually impossible to achieve the necessary temperature that quantum fluctuations are dominated.

### B. Quench from or to the critical point

The time evolution of REC, $Cl_1$, QFI, and LQC are plotted for a quench to the critical point $h_1 = 1$ for $h_0 = 0.7$ in Fig. 4, for different system sizes. As is clear, in a very short time all quantities change rapidly from the equilibrium state to their average (constant) value that they oscillate around. More than that, all quantities show suppressions and revivals as deviations from the average value. To study the effect of the system size on revival or suppression time, $t_r$, we also plot

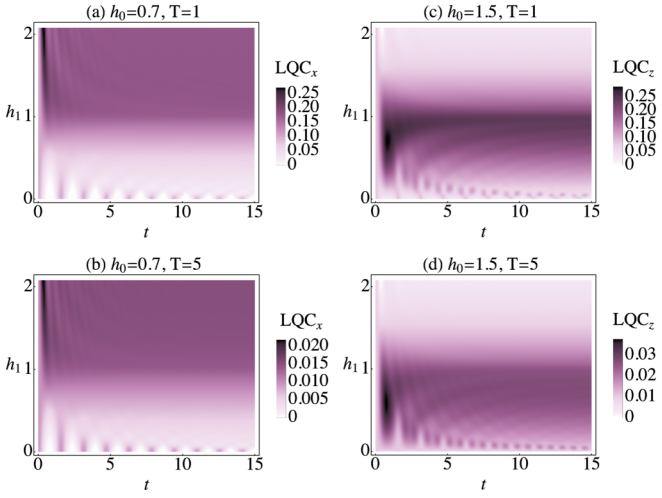


FIG. 3. The density plots of the local quantum coherence versus $t$, and $h_1$, for the different temperatures of $T = 1$ and $T = 5$. Panels (a) and (b) show the $LQC_x$ for $h_0 = 0.7$, and panels (c) and (d) represent the $LQC_z$ for $h_0 = 1.5$.

$t_r(N)$ versus the system size in Fig. 4(f). As seen, the $t_r$ increases linearly with system size, i.e.,

$$t_r(N) = \tau N, \tag{28}$$

where the scaling ratio is obtained as $\tau = 0.2405$. A more detailed analysis shows that $t_r$ and $\tau$ are the same for all quenches and do not depend on the initial preparation phase of system. This is the promised universality of revival or suppression time, which shows that the size of the quench (different values of $h_0$) and the initial phase of the system are unimportant.

We also demonstrate in Fig. 5 the evolution of REC, $Cl_1$, QFI, and LQC for $h_1 = 1.5$ and $h_0 = h_c$, where the system is prepared initially at the critical point. Applying the external magnetic field causes a rapidly change in all quantities from the equilibrium state to a constant value, before starting oscillations at the time $t_c(N)$ [see the insets in Figs. 5(a)–5(e)]. In principle, $t_c(N)$ is an instance time under which all curves correspond to a system larger than size $N$, clearly join together. Examining the details in Fig. 5(f) also shows a linear behavior of $t_c$ versus $N$,

$$t_c(N) = \tau_c N, \tag{29}$$

and interestingly we find a similar scaling value as revival or suppression time; namely, $\tau_c = \tau = 0.2405$. Our calculations show that $t_c$ and $\tau_c$ are the same for all quenches and do not depend on the phase of the system where it quenched to. This is the promised universality of $t_c$ which shows that the size of the quench (different values of $h_1$) and the phase of system, where the system is quenched to, are ineffectual.

Finally, we study the dynamics of REC, $Cl_1$, WYSI, and QFI for anisotropic case $\gamma \neq 0$. Our numerical analyses show that our previous findings are correct for anisotropic case (see Appendix B). It is worthwhile to mention that, for the case $\gamma < 0$, when the system is initialized at the phase with $M^y(t, T = 0) \neq 0$, the critical point of the system is signalled by the maximum of $LQC_y$ (see Appendix B). Moreover, the numerical simulation shows that $t_r$, $t_c$ and their scaling ratios $\tau$ and $\tau_c$ are independent of the anisotropy parameter.

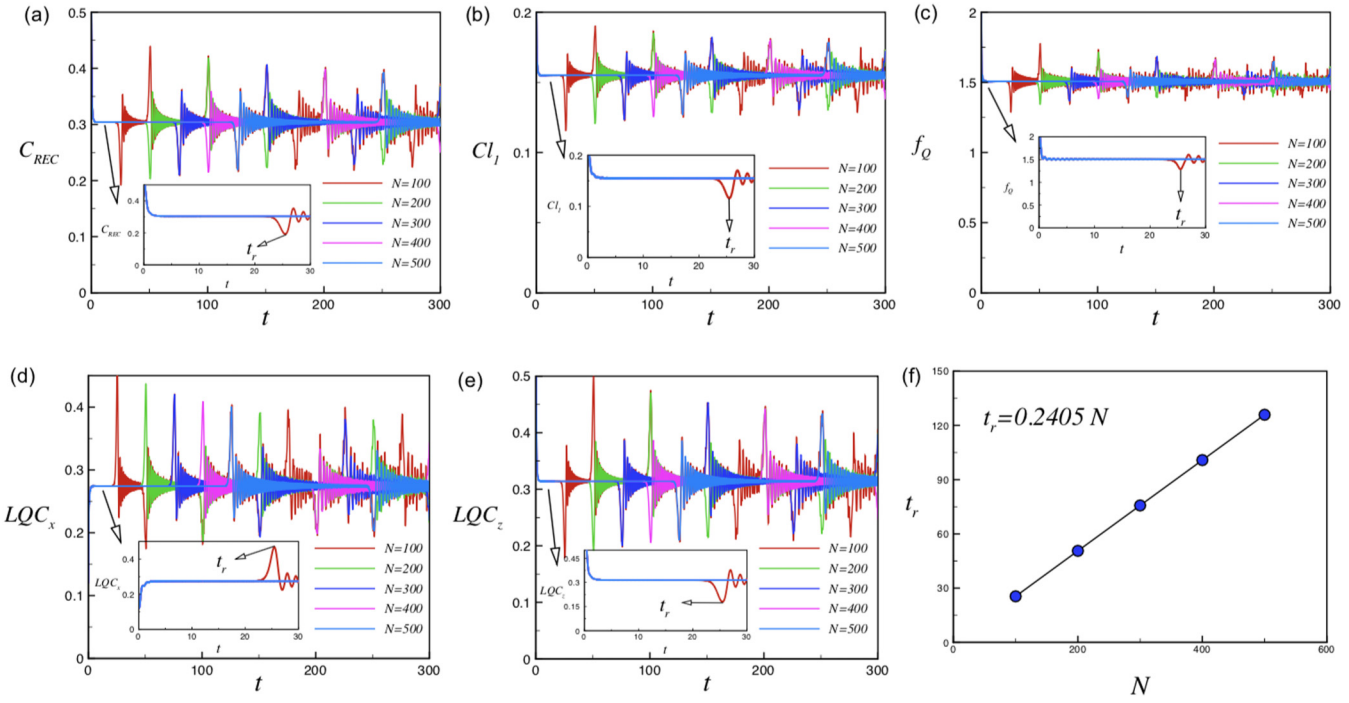


FIG. 4. The evolution of (a) the relative entropy of quantum coherence, (b) the $l_1$ norm of quantum coherence, (c) the quantum Fisher information $\mathcal{F}_Q$, and (d), (e) local quantum coherence, for a quench to the critical point $h_1 = h_c$, for $h_0 = 0.7$ at zero temperature, and for the different system sizes. Panel (f) shows the linear behavior of the first suppression time (revival time) $t_r(N)$ versus the system size.

## V. SUMMARY

We have reported the dynamical behavior of quantum coherence in the one-dimensional time-dependent transverse magnetic field $XY$ model. For this purpose, we investigate the dynamics of relative entropy of coherence, $l_1$ norm of coherence, Wigner-Yanase skew information, and quantum Fisher information. We show that the phase-transition point can be signalled by the maximum of the Wigner-Yanase skew information local components, even at low temperature. The

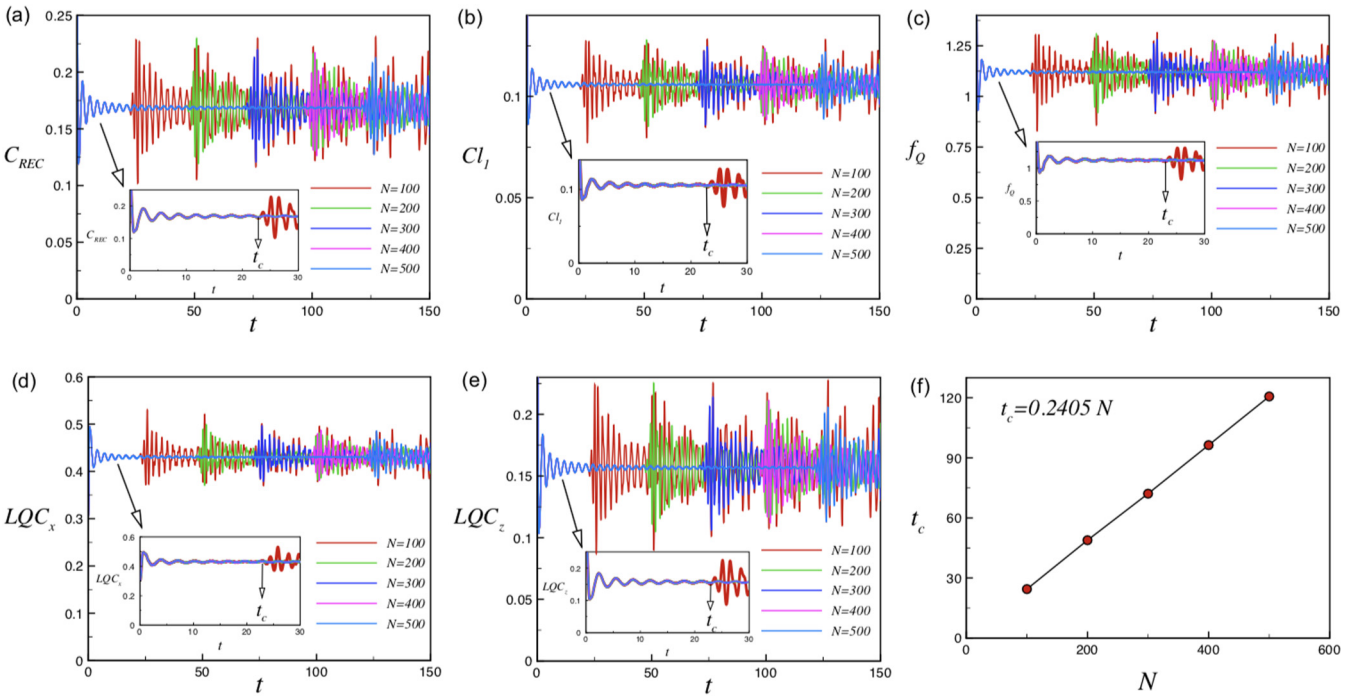


FIG. 5. (a)–(e) The same plots as in Figs. 4(a)–4(e) but for the case that the system is at the critical point $h_0 = h_c$, and quenched to $h_1 = 1.5$. All plots show again an oscillating behavior after time $t_c$, which scales linearly versus the system size shown in panel (f).

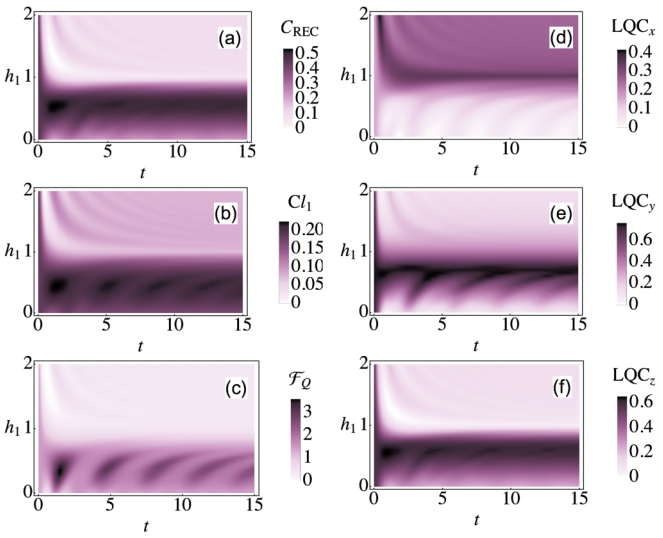


FIG. 6. Same density plots as Fig. 1 but for the case of $\gamma = 0.5$, at zero temperature and for $h_0 = 0.7$ ($h_0 < h_c$).

relative entropy of coherence, $l_1$ norm of coherence, and quantum Fisher information lack such an indicator of criticality in the model. In addition, we find that all of these quantities show suppressions and revivals by quenching the system to the critical point. Furthermore, the first suppression (revival) time scales linearly with system size and free from the quench size and the initial phase of system, therefore our work highlights the universality in out-of-equilibrium quantum many-body systems.

The success of the Wigner-Yanase skew information dynamics to reveal the equilibrium phase transition may originate from its dependence on the square root of the elements of the density matrix. Therefore, it is a meaningful proposal to study the dynamics of similar quantifiers with a functionality of the square root of the elements of the density matrix. Moreover, it will be interesting to extend the current investigation to more general time-dependent cases of the external magnetic field, such as exponential or periodic functions, and also it is worthwhile to extend the calculation to the disorder case.


## ACKNOWLEDGMENTS

We thank U. Mishra for helpful discussions. A.A. acknowledges financial support from the National Research Foundation (NRF) funded by the Ministry of Science of Korea (Grants No. 2016K1A4A01922028, No. 2017R1D1A1B03033465, and No. 2019R1H1A2039733).


## APPENDIX A: TWO-POINT CORRELATION FUNCTIONS OF TIME-DEPENDENT *XY* MODEL

Using Eqs. (6), and (7) the expectation value of the magnetization along the $z$ direction, specifically, is given by [50–54],

$$\langle M^z\rangle = \frac{1}{4N}\sum_{p=1}^{N/2}\frac{\tanh\left[\beta\Gamma(h_0,J_0)\right]}{\Gamma^2(h_1,J_1)\Gamma(h_0,J_0)}\big\{2J_1(J_0h_1-J_1h_0)\delta_p^2 \times \sin^2\left[2t\Gamma(h_1,J_1)\right]+4\Gamma^2(h_1,J_1) \times (J_0\cos\phi_p+h_0)\big\}, \tag{A1}$$

where $\phi_p = 2\pi p/N$, $\delta_p = 2\gamma\sin\phi_p$, and $\beta = 1/K_BT$. Here $K_B$ is the Boltzmann constant and $T$ is the temperature. One can simply use the Wick theorem [67] to obtain the nearest-neighbor spin-correlation functions as follows:

$$\begin{aligned}\left\langle S_l^xS_{l+1}^x\right\rangle &= \tfrac{1}{4}F_{l,l+1},\\ \left\langle S_l^yS_{l+1}^y\right\rangle &= \tfrac{1}{4}F_{l+1,l},\\ \left\langle S_l^zS_{l+1}^z\right\rangle &= \tfrac{1}{4}[F_{l,l}\times F_{l+1,l+1}-Q_{l,l+1}\times G_{l,l+1}\\ &\quad -F_{l+1,l}\times F_{l,l+1}],\end{aligned} \tag{A2}$$

in which by defining $\Gamma[h(t),J(t)] = \{[J(t)\cos\phi_p+h(t)]^2+\gamma^2J^2(t)\sin^2\phi_p\}^{\frac{1}{2}}$, we can write

$$Q_{l,m} = \frac{1}{N}\sum_{p=1}^{N/2}\left[2\cos[(m-l)\phi_p]+\frac{i(J_1h_0-J_0h_1)\delta_p\sin[(m-l)\phi_p]\sin\left[4t\Gamma(h_1,J_1)\right]\tanh\left[\beta\Gamma(h_0,J_0)\right]}{\Gamma(h_1,J_1)\Gamma(h_0,J_0)}\right],$$

$$G_{l,m} = \frac{1}{N}\sum_{p=1}^{N/2}\left[-2\cos[(m-l)\phi_p]+\frac{i(J_1h_0-J_0h_1)\delta_p\sin[(m-l)\phi_p]\sin\left[4t\Gamma(h_1,J_1)\right]\tanh\left[\beta\Gamma(h_0,J_0)\right]}{\Gamma(h_1,J_1)\Gamma(h_0,J_0)}\right],$$

$$\begin{aligned}F_{l,m} = \frac{1}{N}\sum_{p=1}^{N/2}\frac{\tanh\left[\beta\Gamma(h_0,J_0)\right]}{\Gamma^2(h_1,J_1)\Gamma(h_0,J_0)}\big[&\cos[(m-l)\phi_p]\big\{J_1[J_0h_1-J_1h_0]\delta_p^2\sin^2\left[2t\Gamma(h_1,J_1)\right]+2\Gamma^2(h_1,J_1)(J_0\cos\phi_p+h_0)\big\}\\ &+\delta_p\sin[(m-l)\phi_p]\{J_0\Gamma^2(h_1,J_1)+2(J_1h_0-J_0h_1)(J_1\cos\phi_p+h_1)\sin^2\left[2t\Gamma(h_1,J_1)\right]\}\big].\end{aligned} \tag{A3}$$

## APPENDIX B: WIGNER-YANASE SKEW INFORMATION FOR ANISOTROPIC CASE $\gamma \neq 0$

In this Appendix, we study the dynamics of the quantities for anisotropic case $\gamma \neq 0$ [Eq. (1)]. For this purpose, in Fig. 6, we first look at the anisotropic case $\gamma = 0.5$. We show the density plot of dynamical behavior of the relative entropy of coherence [Fig. 6(a)], the $l_1$ norm of coherence [Fig. 6(b)], the quantum Fisher information [Fig. 6(c)], and local quantum coherence components [Figs. 6(d)–6(f)], versus time and $h_1$, for $J_0 = J_1 = 1$, and $h_0 = 0.7$. As we expect, when the initial state prepared in the ferromagnetic case $M^x \neq 0$, the $\mathrm{LQC}_x$ shows maximum at the critical point of the system $h_c = 1$. Moreover, we show that, when the system initialized at the paramagnetic phase $M^z \neq 0$, i.e., $h_0 > 1$, the $\mathrm{LQC}_z$ fulfils the

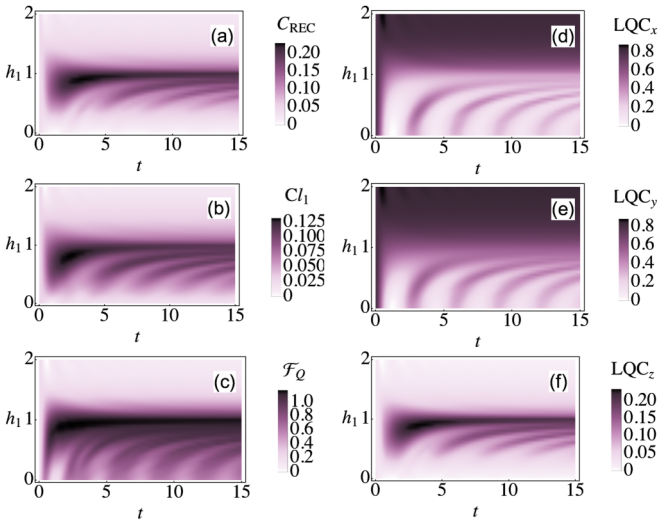


FIG. 7. Same density plots as Fig. 1 but for the case of $\gamma = 0.5$ at zero temperature and $h_0 = 1.5$ ($h_0 > h_c$).

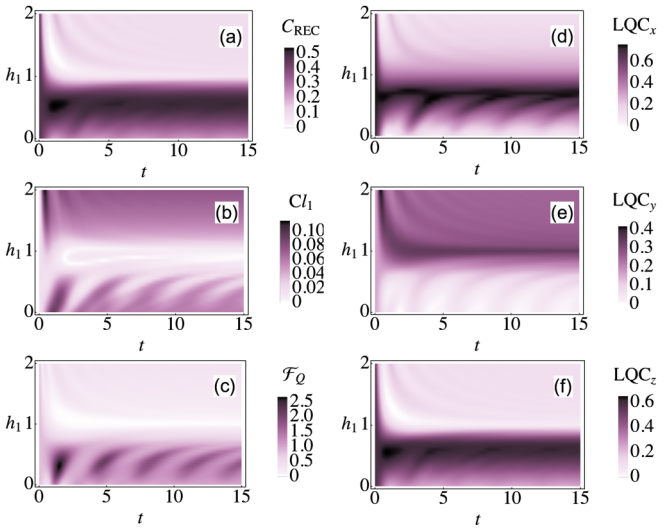


FIG. 8. Same density plots as in Fig. 1 but for the case of $\gamma = -0.5$ at zero temperature and $h_0 = 0.7$ ($h_0 < h_c$) with magnetization along the $y$ direction.

expectation and reaches its maximum at the critical point. This is clearly represented in the results of Fig. 7. Finally, for the case in which the system is initially prepared in the ferromagnetic phase $\gamma < 0$ and in which $M^y \neq 0$, the maximum of $\mathrm{LQC}_y$ happens at the critical point of the system (see Fig. 8). Briefly, one can conclude that, when the system is prepared in the initial state with $M^\alpha \neq 0$, the dynamics of $\mathrm{LQC}_\alpha$ reaches its maximum value at the critical point.


[1] R. Horodecki, P. Horodecki, M. Horodecki, and K. Horodecki, Rev. Mod. Phys. **81**, 865 (2009).
[2] K. Modi, A. Brodutch, H. Cable, T. Paterek, and V. Vedral, Rev. Mod. Phys. **84**, 1655 (2012).
[3] Z. Ficek and S. Swain, *Quantum Interference and Coherence* (Springer-Verlag, New York, 2005).
[4] I. Chuang and M. Nielsen, *Quantum Computation and Quantum Information* (Cambridge University Press, Cambridge, 2000).
[5] T. Baumgratz, M. Cramer, and M. B. Plenio, Phys. Rev. Lett. **113**, 140401 (2014).
[6] Z. Xi, Y. Li, and H. Fan, Sci. Rep. **5**, 10922 (2015).
[7] M.-L. Hu and H. Fan, Sci. Rep. **6**, 29260 (2016).
[8] M. Qin, Z. Ren, and X. Zhang, Phys. Rev. A **98**, 012303 (2018).
[9] L. Balazadeh, G. Najarbashi, and A. Tavana, Quantum Inf. Process. **19**, 181 (2020).
[10] S. Rana, P. Parashar, and M. Lewenstein, Phys. Rev. A **93**, 012110 (2016).
[11] D. Girolami, Phys. Rev. Lett. **113**, 170401 (2014).
[12] J.-F. Huang, Y. Li, J.-Q. Liao, L.-M. Kuang, and C. P. Sun, Phys. Rev. A **80**, 063829 (2009).
[13] Z. Huang, Quantum Inf. Process. **16**, 207 (2017).
[14] S. Lei and P. Tong, Quantum Inf. Process. **15**, 1811 (2016).
[15] Z. Mzaouali and M. E. Baz, Phys. A (Amsterdam, Neth.) **518**, 119 (2019).
[16] E. P. Wigner and M. M. Yanase, Proc. Natl. Acad. Sci. U. S. A. **49**, 910 (1963).
[17] S. Luo, Phys. Rev. Lett. **91**, 180403 (2003).
[18] R. A. Fisher, Math. Proc. Cambridge Philos. Soc. **22**, 700 (1925).
[19] C. W. Helstrom, *Quantum Detection and Estimation Theory*, Math. Sci. Eng. (Academic Press, New York,1976).
[20] B. R. Frieden and B. H. Soffer, Phys. Rev. E **52**, 2274 (1995).
[21] B. R. Frieden, Am. J. Phys. **68**, 1064 (2000).
[22] Y.-R. Zhang, Y. Zeng, H. Fan, J. Q. You, and F. Nori, Phys. Rev. Lett. **120**, 250501 (2018).
[23] M. M. Taddei, B. M. Escher, L. Davidovich, and R. L. de Matos Filho, Phys. Rev. Lett. **110**, 050402 (2013).
[24] P. Gibilisco, D. Imparato, and T. Isola, J. Math. Phys. **48**, 072109 (2007).
[25] G. Karpat, B. Çakmak, and F. F. Fanchini, Phys. Rev. B **90**, 104431 (2014).
[26] C. Invernizzi, M. Korbman, L. C. Venuti, and M. G. A. Paris, Phys. Rev. A **78**, 042106 (2008).
[27] Z. Sun, J. Ma, X.-M. Lu, and X. Wang, Phys. Rev. A **82**, 022306 (2010).
[28] A. S. Holevo, *Probabilistic and Statistical Aspects of Quantum Theory*, Math. Sci. Eng. (Edizioni della Normale, New York,1982).
[29] S. L. Braunstein and C. M. Caves, Phys. Rev. Lett. **72**, 3439 (1994).
[30] S. L. Braunstein, C. M. Caves, and G. Milburn, Ann. Phys. (NY) **247**, 135 (1996).
[31] J. Wang, Z. Tian, J. Jing, and H. Fan, Phys. Rev. A **93**, 062105 (2016).
[32] X. Liu, Z. Tian, J. Wang, and J. Jing, Ann. Phys. (NY) **366**, 102 (2016).
[33] X. Hu, Phys. Rev. A **94**, 012326 (2016).

[34] Y. Yao, G. H. Dong, X. Xiao, and C. P. Sun, Sci. Rep. **6**, 32010 (2016).
[35] M. Hillery, Phys. Rev. A **93**, 012111 (2016).
[36] J. Ma, B. Yadin, D. Girolami, V. Vedral, and M. Gu, Phys. Rev. Lett. **116**, 160407 (2016).
[37] J. M. Matera, D. Egloff, N. Killoran, and M. B. Plenio, Quantum Sci. Technol. **1**, 01LT01 (2016).
[38] V. Giovannetti, S. Lloyd, and L. Maccone, Phys. Rev. Lett. **96**, 010401 (2006).
[39] A. Polkovnikov, K. Sengupta, A. Silva, and M. Vengalattore, Rev. Mod. Phys. **83**, 863 (2011).
[40] S. Pappalardi, A. Russomanno, A. Silva, and R. Fazio, J. Stat. Mech.: Theory Exp. (2017) 053104.
[41] J. Häppölä, G. B. Halász, and A. Hamma, Phys. Rev. A **85**, 032114 (2012).
[42] R. Jafari and H. Johannesson, Phys. Rev. Lett. **118**, 015701 (2017).
[43] R. Jafari and H. Johannesson, Phys. Rev. B **96**, 224302 (2017).
[44] R. Jafari, H. Johannesson, A. Langari, and M. A. Martin-Delgado, Phys. Rev. B **99**, 054302 (2019).
[45] U. Mishra, H. Cheraghi, S. Mahdavifar, R. Jafari, and A. Akbari, Phys. Rev. A **98**, 052338 (2018).
[46] R. Jafari, Sci. Rep. **9**, 1 (2019).
[47] R. Jafari and A. Akbari, Europhys. Lett. **111**, 10007 (2015).
[48] R. Jafari, Phys. Rev. A **82**, 052317 (2010).
[49] R. Jafari, J. Phys. A: Math. Theor. **49**, 185004 (2016).
[50] E. Barouch, B. M. McCoy, and M. Dresden, Phys. Rev. A **2**, 1075 (1970).
[51] E. Barouch and B. M. McCoy, Phys. Rev. A **3**, 786 (1971).
[52] G. Sadiek, B. Alkurtass, and O. Aldossary, Phys. Rev. A **82**, 052337 (2010).
[53] Z. Huang and S. Kais, Phys. Rev. A **73**, 022339 (2006).
[54] U. Mishra, D. Rakshit, and R. Prabhu, Phys. Rev. A **93**, 042322 (2016).
[55] A. Streltsov, G. Adesso, and M. B. Plenio, Rev. Mod. Phys. **89**, 041003 (2017).
[56] B. Çakmak, G. Karpat, and Z. Gedik, Phys. Lett. A **376**, 2982 (2012).
[57] N. Li and S. Luo, Phys. Rev. A **88**, 014301 (2013).
[58] A. W. Chin, S. F. Huelga, and M. B. Plenio, Phys. Rev. Lett. **109**, 233601 (2012).
[59] J. Liu, X. Jing, and X. Wang, Phys. Rev. A **88**, 042316 (2013).
[60] Y. M. Zhang, X. W. Li, W. Yang, and G. R. Jin, Phys. Rev. A **88**, 043832 (2013).
[61] P. Pfeuty, Ann. Phys. (NY) **57**, 79 (1970).
[62] B. M. McCoy, Phys. Rev. **173**, 531 (1968).
[63] T. J. Osborne and M. A. Nielsen, Phys. Rev. A **66**, 032110 (2002).
[64] S. L. Sondhi, S. M. Girvin, J. P. Carini, and D. Shahar, Rev. Mod. Phys. **69**, 315 (1997).
[65] M. C. Arnesen, S. Bose, and V. Vedral, Phys. Rev. Lett. **87**, 017901 (2001).
[66] D. Gunlycke, V. M. Kendon, V. Vedral, and S. Bose, Phys. Rev. A **64**, 042302 (2001).
[67] G. C. Wick, Phys. Rev. **80**, 268 (1950).